JOURNAL OF THE KOREAN ASTRONOMICAL SOCIETY
33: 97 ~ 110, 2000

ABUNDANCES OF PLANETARY NEBULAE IN M 31 AND M 32

SIEK HYUNG[1], LAWRENCE H. ALLER[2], SOO-RYEON HAN[3], YOUNG-KWANG KIM[1], WONYONG HAN[1], AND YOUNGJUN CHOI[1]
[1]Korea Astronomy Observatory
[2]Dept. of Physics and Astronomy, UCLA, CA 90095, U.S.A.
[3]Dept. of Earth Science Education, Korea National University of Education
E-mail: hyung@kao.re.kr, aller@astro.ucla.edu, and srhan,glory,whan,cschoi@kao.re.kr
(Received Aug. 30, 2000; Accepted Sep. 18, 2000)

ABSTRACT

Planetary nebulae provide a direct way to probe elemental abundances, their distributions and their gradients in populations in nearby galaxies. We investigate bulge planetary nebulae in M 31 and M 32 using the strong emission lines, Hα, He I, [O III], [N II], [S II] and [Ne III]. From the [O III] 4363/5007 line ratio and the [O II] 3727/3729, we determine the electron temperatures and number densities. With a standard modeling procedure (Hyung, 1994), we fit the line intensities and diagnostic temperatures, and as a result, we derive the chemical abundances of individual planetary nebulae in M 31 and M 32. The derived chemical abundances are compared with those of the well-known Galactic planetary nebulae or the Sun. The chemical abundances of M 32 appear to be less enhanced compared to the Galaxy or M 31.

Key words : ISM : galaxies (M 31, M 32) – planetary nebulae : photoionization model : chemical abundance

I. INTRODUCTION

Using the Palomar 5-m telescope with photographic plates and a 1500 Å broad-band filter, Baade (1955) was the first person to identify planetary nebulae (PNs) in M 31 (Andromeda galaxy). Later, Ciardullo, Jacoby and their colleagues (1978, 1989) detected a total of about 600 PNs ($20.5 \leq m_{\rm m5007} \leq 24$, where $m_{\rm m5007} = -2.5 \log F_{\rm m5007} - 13.74$) of which main purpose is to derive the distance to M 31 using a PN luminosity function. The brightest PN of M 31 is of $m_{\rm m5007} \sim 20.45$.

Since the pioneering work by Spinrad & Taylor (1971, hereafter ST71) on the optical spectra of M 31's bulge [angular diameter ~240′, RA=0^h42^m and Decl.= +41°16′ (2000), E(B-V) ~ 0.12], the integrated spectroscopy seemed to suggest that the cores of giant E/S0 galaxies and the bulges of large spirals contain a significant population of metal-enriched star (e.g., Worthey, Faber, & Gonzalez 1992, hereafter WFG). Abundance determinations based on the strength of stellar absorption lines using synthesis techniques, are limited by velocity broadening in the galaxies, though.

Utilizing the emission spectra of PNs or H II regions would be one of the most precise and direct way to determine the chemical abundances of the nearby galaxies. From observed emission line strengths of He, N, O, Ne and S in the extra galactic H II regions, abundance gradients in spiral galaxies are well established, i.e. decreasing O/H with galactocentric distance (see Pagel & Edmunds 1981; Walsh & Roy 1989). However, H II regions are not found throughout the whole galaxy.

In contrast to H II regions, PNs do not belong to any single stellar population, and are found throughout a galaxy. Although some of elements are affected by internal chemical processing of an evolution, important elements, such as O, Ne, Ar and S, are generally believed to be unaffected by this process. PNs are ideal tools for obtaining the metallicity, as they are useful in measuring the abundance gradients from the very center of the galaxy to the outer most regions via a single analysis technique. However, there is little spectroscopic data in the nearby galaxies, except for M 31 and M 32 (distance ~ 2.9 Mpc for both) by Jacoby & Ciardullo (1999) and by Richer, Stasinska, & McCall (1999, RSM hereafter). These authors used the Kitt Peak 4-m (with the slit masks on the Ritchey-Chretien spectrograph) and CFHT 3.5-m (with the focal plane mask on the MOS) telescopes to obtain somewhat detailed spectra of about 15 PNs for He, C, N, O, Ne, S, Ar abundance study and limited spectra of 30 PNs for O abundance study, respectively.

Recently, Walsh et al. (1999) derived abundances for 5 PNs in the nearby galaxy Centaurus A (NGC 5128, 4 times farther than M 31), using the ESO 3.6-m telescope. The PNs in the Centaurus A by Walsh et al. are 2–3 magnitude fainter than those in M 31. This demonstrates the 2–4 m telescopes would be useful to study the PNs in closer dwarf galaxies. In this investigation, we try to find the physical conditions of 30 PNs of M 31 and 9 PNs of M 32 utilizing the spectroscopic data secured with the CFHT/MOS (RSM). We also try to derive the chemical abundances of PNs in M 32 using a photoionized model approach (Hyung 1994; Hyung & Aller 1996). We compare these abundances with those of Galactic PNs and briefly discuss

the chemical evolutionary status of M 32 and M 31.

II. SPECTRAL DATA AND DIAGNOSTICS

Since M 31 and M 32 are relatively distant, it will be hard to obtain the high dispersion spectrum even with the currently available large telescope, so the data we are dealing, here, are those of medium dispersion spectrometer. The emissions are relatively weak and subject to a large error. Fortunately, the extinction of PNs in M 31 is relatively small, i.e. E(B-V) $\simeq$ 0.01, while that of PNs in M 32 is quite large, i.e., E(B-V) $\simeq 0.3 \sim 0.5$.

The spectral data observed by RSM present numerous spectral lines (corrected for the interstellar extinction). There are not very many spectral lines available for PNs in M 31, though. RSM's spectral observations of M 32 cover a wider wavelength range than those of M 31 by Jacoby & Ciardullo. Thus, the emission lines of [S II] 6716, 6730 and [Ar III] 7136 are also available in the M 32 spectral data. The strongly observed emission lines are those of [O III] 4959, 5007, Hα, [N II] 6548, 6584, and [Ne III] 3869, 3967. We use the line intensities, given on the scale of I(Hβ) = 100.0 by RSM for our model studies.

We are able to derive the electron temperatures of PNs from the [O III] 4363/(4959+5007) line ratios. However, the [S II] 6716/6730 and [O II] 3726/3729 line ratios, which are useful for the density determination, are available for a few PNs only. With the correct atomic constants, we are able to obtain the electron temperature correctly but not possible for the electron density. The atomic constants of a recent compilation of electronic collision strengths and atomic transition probabilities are found in Hyung and Aller (1996).

Fig. 1 gives the temperature diagnostic diagram for PNs in M 31. We found diversified temperatures in 30 PNs listed in the RSM. The highest temperature is 15 000 K and the lowest value is 9 400 K. In Table 1, we compare the diagnostic temperatures of M 31 PNs, derived by RSM and by us: consecutive columns present the target name assigned by Ciardullo et al. (1989, hereafter CJFN), the diagnostic electron temperatures by RSM, our derivations and the summed O^+,O^{++} ionic concentrations by RSM. The electron temperatures were derived assuming the electron number density, 4000 cm^{-3} for both RSM and ours. In certain occasions, [O III] 4363 lines were too weak to detect, so one can set the upper limits only. These were given by RSM in column (2). We did not indicate the observational errors in Col. (3), which would be the same amount as in RSM.

Our derivations do not differ largely from those by RSM except for PN48, for which our diagnostic indication of temperature is higher, i.e. 10 300 K (ours) vs. 9500 K (RSM). There appears to be accidental errors involved in RSM. For others, the discordance between two investigations seems negligible. The small amount of discordances must be coming from different atomic constants employed in both.

Note that there appears to be a gap between represented by [O III] electron temperatures. We subdivided the M 31 PNs into three groups according to the excitation temperatures. 1) The first group consists of 3 low excitation PNs of lowest electron temperatures, i.e. T([O III]) $\sim$ 9500 K. Very roughly speaking, 30% of the M 31 PNs are of relatively low excitation. Existence of these relatively low temperature PNs seems interesting, considering the fact that one must observe only high excitation PNs in the extra galaxies. 2) The second group of PNs shows the moderately high electron temperature, i.e. T_e = 13 000 K. 3) The 3rd group is the high excitation PNs of $T_e \sim$ 15 000 K.

Table 1. Diagnostics of PNs in M 31

Name	T_e^a(K)	T_e^b(K)	12+log(O/H)
PN1	<10100		>8.79
PN3	<9400		>8.96
PN4	<12200		>8.58
PN10	<13600		>8.22
PN12	13100±2000	13000	8.44±0.18
PN17	<18400		>7.84
PN23	<13200		>8.30
PN28	<8600		>9.11
PN29	<9800		>8.91
PN30	<9300		>9.00
PN31	10700±780	10600	8.80±0.10
PN36	14600±1600	14400	8.12±0.12
PN38	<10500		>8.58
PN42	12400±750	12500	8.57±0.08
PN43	<10200		>8.71
PN45	15100±940	15000	8.16±0.07
PN47	9600±1200	9500	8.77±0.20
PN48	9500±640	10300	8.95±0.11
PN52	<11300		>8.53
PN53	9600±870	9600	8.91±0.14
PN80	<9500		>8.91
PN91	12700±1400	12700	8.38±0.13
PN92	11800±1100	11700	8.56±0.12
PN93	<10500		>8.79
PN95	<9300		>8.66
PN97	9400±1000	9400	8.87±0.18
PN172	13100±1100	13100	8.44±0.10
PN380	13900±1100	13900	8.38±0.09
PN387	10600±810	10400	8.71±0.12
PN408	<13000		>8.52

[a]: Col. (2) : M. G. Richer, G. Stasinska, & M. L. McCall (1999, RSM). [b]: our derivation: Col. (4) : summation of O^+ and O^{++} ionic abundances. < and > mean the upper and low limits due to the faintly observed [O III] λ 4363 line.

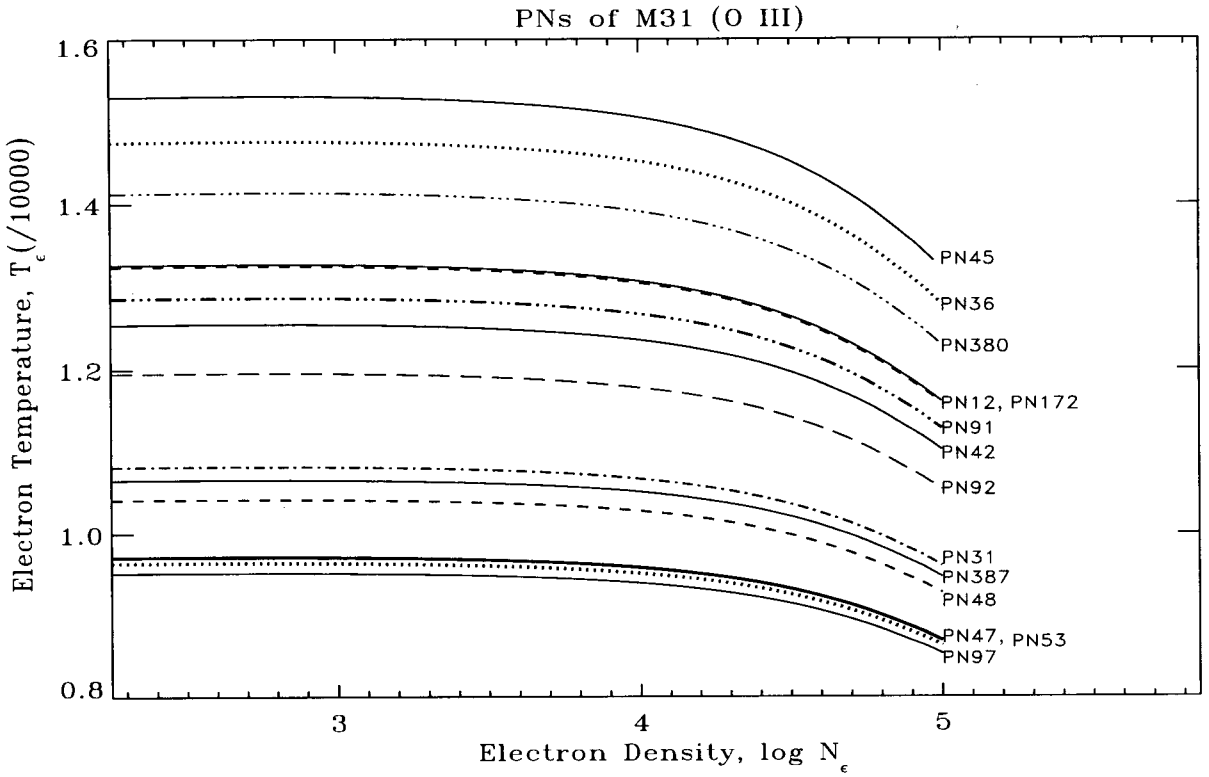

Fig. 1.— [O III] electron temperatures of PNs in M 31.

Fig. 2 shows the diagnostics of PNs in M 32, and their values are listed in Table 2. Note that the electron number densities are available for the case of M 32, since the [S II] and [O II] spectral lines were secured. The [Ar III] lines, which would be useful for Ar abundance determination, are also available. Since the numerous lines are available, with the photoionization model we will be able to derive the chemical abundance more accurately, here. Whereas, the abundance determination of M 31 PNs will be very coarse and therefore, any further discussions would be pointless.

The electron number densities suggested by [S II] are fairly low, 3200 cm^{-3} ($\log N_e \sim 3.5$) and the [O II] suggests even lower density $<1000\ cm^{-3}$ in M 32 PNs. The highest electron temperature of PNs in M 32 is 18 500 K (PN24), which is 3000 K higher than the M 31 PN45's electron temperature. This is unlikely due to a biased sampling – For the M 32 PN observation, which is relatively smaller in size than M 31 (8×6″ vs. 178×63″), only highest excitation M 32 PNs had been observed by RSM. Note that the lowest electron temperature of M 32 PN is also fairly high, i.e., T_e = 12 000 K. May this higher electron temperature be caused by a lower chemical abundance in M 32 PNs?

The diagnostics (or physical conditions) of the M 31 and M 32 PNs can be compared with those of the well-known Galactic PNs. As mentioned above, all of the observed PNs in M 31 and M 32 are probably of high ex-

Table 2.- Diagnostics of PNs in M 32

Name	T_e^a(K)	T_e^b(K)	N_e	[O/H]
PN1	<11500	12000	4200	>8.39
PN2	<15700	12000	3200	>8.17
PN5	11800±1300	11600	10000	8.43±0.16
PN6	12700±2500			8.46±0.27
PN7	<13400			>8.08
PN8	13000±1400	13000	3200	8.36±0.14
PN11	<25300	12000	2000	>7.25
PN24	18200±2500	18300	10000	8.07±0.13
PN25	<18600			>8.02

Cols. (2) and (5) : M. G. Richer, G. Stasinska, & M. L. McCall (1999) a : Electron temperature and upper limit, determined using the upper limit of [O III] λ 4363 Col. (5) : 12+log(O/H). Here, [O/H] means O^+ and O^{++} ionic abundances. Cols. (3) & (4) : Electron temperatures and densities derived using the plasma diagnostics.

citation, since one can observe only the brightest PNs in the extra galaxies. The electron temperatures of Galactic PNs are ranging from 9600 to 17 500 K (see Table 3 in Section 3). The highest temperature of M 31 PN is still lower than that of M 32 PN or the Galactic PN. Relatively lower electron temperature in M 31 PN suggests the chemical abundance of M 31 is perhaps enhanced compared to the Galaxy. We must postpone our conclusion till we find the PN abundances of M 31 and M 32 in the following photoionization model investigation, though.

III. MODELS AND ABUNDANCES

Since the observations were done for the whole image of each PN (i.e., the PNs are smaller than the employed slit size in the observations), the spectral data represent the whole structure of PN. It would be useless to construct an elaborate 2-dimensional or 3-dimension model for a point source object which does not have any structural information to justify. Thus, we simply employ a spherically symmetrical structure in a nebular geometry. The spherically symmetrical geometry had been used in many photoionization model studies by most workers; and this had been a first approximation in Hyung et al.'s studies (see Hyung & Aller 1996). A description of the employed modeling procedures may be found in Hyung (1994) and a later update can be found in Hyung and Aller (1996). The atomic parameters are constantly updated in a code.

In the photoionization model investigation, one must fit not only the line intensities but the diagnostics temperature. Only if proper chemical abundances are introduced as an input, the predicted electron temperature will be close to the observed. Thus, the diagnostic temperatures serve as a constraint for modeling studies. It would be hard to understand if one can predict the line intensities well simultaneously with two or more independent models where radically different effective temperatures are employed for the central star. However, according to Hyung et al.'s Galactic PN investigation, only one model can predict the line intensities and the average electron temperature at the same time.

Table 3 gives a summary of the Galactic PN spectral investigation based on high dispersion spectroscopies of Hamilton Echelle Spectrograph (HES) at the Lick 3-m telescope (Hyung et al. 1994–2000). The predicted electron temperatures by Hyung et al.'s modeling studies seemed to show a deviation of less than ±500 K between the predicted and the observed [O III] electron temperatures. Thus, the Galactic PNs' electron temperature in col. (2) of Table 3 might be close to the observed values of bright Galactic PNs within the observational errors. The 3rd column lists the effective temperature of the central star (indicated by theoretical model by Hyung et al.). There are many diversified central stars, i.e. 29 000 ~ 180 000 K and these can be used as standards for extra galactic PN investigation. We use the data in Table 1 as a guideline of M 32 PNs' modeling. Col. (4) of Table 3 lists the logarithmic value of central star gravity adopted in a theoretical model; and the remaining columns are helium abundance ratio relative to hydrogen; central stellar radius; inner and outer shell radii. The last column indicates whether Hyung et al. employed local thermal equilibrium (LTE) or non-LTE model atmospheres.

As in our previous modeling effort of the Galactic PNs, we introduce a central star energy distribution generated from Hubeny's (1988) non-LTE model atmospheres. The choice of model atmosphere for the central star fixes the level of excitation of the spectrum. Thus, we need to test various model atmospheres, corresponding to different stellar effective temperatures till the model prediction gives the right excitation, e.g. He I, He II, [O II] and [O III]. For all PNs, we assumed that in the radiating strata, the dust to gas ratio, $M_{dust}/M_{gas} = 0.005$: the internal dust influence would be negligible in the intensity prediction. The detailed dust influence on the lines is beyond the scope of our concern, here. Shock heating is not included in this model construction.

Since a small number of lines in the wavelength of 3800 – 6600 (7200) Å are available for M 31 PNs, modeling effort would not be so helpful for M 31. Thus, we present the results only for a few PNs in M 31, i.e., PN47, PN97, PN387, and PN17. Table 4-1 and 4-2 show the result. The 3rd and 6th columns give the observed intensities, while the 4th, 5th, 7th and 8th columns present the model predictions. For some PNs, PN47, PN97 and PN387, one cannot find a single satisfactory model for the observed spectrum. Thus, we list two model predictions. For PN17, we are able to find a single satisfactory model.

To determine the chemical abundances empirically, one must estimate the ionic abundances in the unobserved ionization stage. For O, RSM used an empirical ionization correction factor (ICF), adopted from Kingsburgh & Barlow (1994, hereafter KB). The O abundances empirically determined by RSM agree with ours within a factor of 2 except for PN17. PN17 is a background object (Ford & Jenner 1975). PN17 is largely uncertain because the electron temperature information is not available from the diagnostics: RSM used the uncertain value, while we are totally dependent on the model prediction.

The most abundant elements in PNs are those of He, C, N, O, Ne, and S. Unfortunately, carbon spectral lines are not available in the optical wavelength region. For the unobserved carbon, we assumed a certain amount of carbon in a model input, i.e., 5(−5) or 6(-6) [here, 5(-5) means 5×10^{-5}]. In the last column of Table 4-2, we also list the average abundaces of Galactic PNs by Kingsburgh & Barlow (1994). The predicted values are given in columns (4), (5), (7) and (8) of Table 4. Our models seem generally successful in fitting the observed line intensities and electron temperatures well.

Our limited sample 4 PNs show that the chemical

Table 3.- Modeling Parameters for Galactic PNs

Object	T_e [K]	T_{eff} [K]	log g	He/H	R_* [$R_\odot$]	R_i [pc]	R_o [pc]	
IC 2149	9700	35000	4.0	0.10	1.2	0.035	0.045	non-LTE
IC 418	10250	29300	3.4	0.07	2.1	0.001	0.0075	LTE
Hubble12	12200	35000	5.5	0.10	3.0	0.005	0.00516	LTE
NGC6543	9600	48000	6.9		0.82	0.026(e)	0.052	non-LTE
NGC6572	10940	50000	5.5	0.10	0.823	0.01(e)	0.0244	non-LTE
IC 4997	11780	55000	5.5	0.14		0.0005	0.013	non-LTE
NGC7009	9840	80000	4.99	0.0967	0.13	0.031	0.0344	non-LTE
NGC6790	10010	85000	5.5	0.11	0.35	0.005(e)	0.018	non-LTE
NGC7662	13000	105000	5.7	0.093	0.15	0.025(e)	0.035	non-LTE
NGC6818	11600	140000	7.8	0.105	0.1	0.0720(e)	0.080	non-LTE
IC 2165	13400	140000	5.5		0.006	0.035	0.059	non-LTE
NGC6886	13000	150000	6.5	0.095	0.046	0.001	0.0345	non-LTE
NGC6741	12540	140000	5.84	0.11	0.063		0.043	non-LTE
NGC2440	14000	180000	6.7	0.11	0.038	0.015	0.0425	non-LTE
NGC6537	17500	180000	6.0	0.13	0.01	0.022	0.041	non-LTE

IC 2149 : Feibelman, Hyung, & Aller (1994); IC 418 : Hyung, Aller, & Feibelman (1994); Hubble12 : Hyung, & Aller (1996); NGC6543 : Hyung et al. (2000); NGC6572 : Hyung, Aller, & Feibelman (1994); IC 4997 : Hyung, Aller, & Feibelman (1994); NGC7009 : Hyung, & Aller (1995); NGC6790 : Aller et al. (1996); NGC7662 : Hyung & Aller (1997); NGC6818 : Hyung, Aller, & Feibelman (1999); IC 2165 : Hyung (1994); NGC6886 : Hyung, Keyes, & Aller (1995); NGC6741 : Hyung, & Aller (1997); NGC2440 : Hyung & Aller (1998); NGC6537 : Hyung (1999)

Table 4-1.— Model predictions for PNs in M 31

Element	Wave	I_{obs}(PN47)	I_{cal1}	I_{cal2}	I_{obs}(PN97)	I_{cal1}	I_{cal2}	Galactic PNs
He I	5876	20.9	20.23	20.14	22.7	21.34	21.35	
N II	6584				35.8	35.85	35.48	
	6548				12.0	12.37	12.25	
O III	4363	8.1	11.47	8.08	9.3	7.81	7.71	
	4959	474	474.21	504.79	565	564.74	560.94	
	5007	1452	1366.00	1454.10	1744	1627.02	1616.07	
Ne III	3868	63.9	63.94	63.36	79.5	79.45	78.84	
	3969	35.4	19.08	18.90	44.5	23.71	23.53	
RSM	T_e	9600±1200			9400±1000			
OURS	T_e	9500			9400			
PNN	R_* ($R_\odot$)		0.50	0.50		0.9	0.9	
	T_* (K)		63000	63000		70000	70000	
	log g		5.5	5.5		6.0	6.0	
Shell (pc)	R_{in}		0.005	0.005		0.023	0.023	
	R_{out}		0.045	0.045		0.083	0.083	
Prediction	T_e		10500	9200		8900	8900	
	N_H		8000	8000		9000	9000	
Chemical	He		1.30(-1)	1.33(-1)		1.40(-1)	1.40(-1)	**1.11(-1)**
Abundance	C		5.00(-5)	–		6.00(-5)	–	**6.48(-4)**
	N		9.00(-5)	–		8.30(-5)	8.20(-5)	**1.40(-4)**
	O	6.0(-4)	4.00(-4)	6.45(-4)	7.6(-4)	9.10(-4)	–	**1.25(-4)**
	Ne		3.92(-5)	6.50(-5)		9.65(-5)	–	**2.42(-6)**

Table 4-2.— Model predictions for PNs in M 31

Element	Wave	I_{obs}(PN387)	I_{cal1}	I_{cal2}	I_{obs}(PN17)	I_{cal1}	Galactic PNs
He I	5876	16.1	16.17	16.17	13.0	13.07	
He II	4686	15.3	15.81	15.84			
N II	6584				77.3	76.74	
	6548				26.3	26.49	
O III	4363	12.3	14.66	14.34			
	4959	525	552.53	549.73	337	335.42	
	5007	1591	1591.40	1583.35	993	966.13	
Ne III	3868	111	111.06	111.14	79	78.30	
	3969	43.9	33.12	33.14			
Ar III	7136				22.5	22.50	
RSM	T_e	10600±810			<18400		
OURS	T_e	10400					
PNN	R_* ($R_\odot$)		0.01	0.01		0.024	
	T_*(K)		140000	140000		180000	
	log g		7.5	7.5		6.0	
Shell (pc)	R_{in}		0.001	0.001		0.020	
	R_{out}		0.050	0.050		0.041	
Prediction	T_e		11000	10900		18100	
	N_H		6000	6000		9000	
Chemical	He		1.13(-1)	1.13(-1)		1.14(-1)	**1.11(-1)**
Abundance	C		6.00(-5)	–		5.00(-5)	**6.48(-4)**
	N		1.50(-6)	1.40(-5)		1.47(-5)	**1.40(-4)**
	O	5.5(-4)	7.94(-4)	8.06(-4)	>4.2(-5)	1.22(-4)	**4.93(-4)**
	Ne		6.37(-5)	6.52(-5)		1.28(-5)	**1.25(-4)**
	Ar					9.80(-7)	**2.42(-6)**

PN17 is a background object in the disk of M 31 (Ford & Jenner 1975)

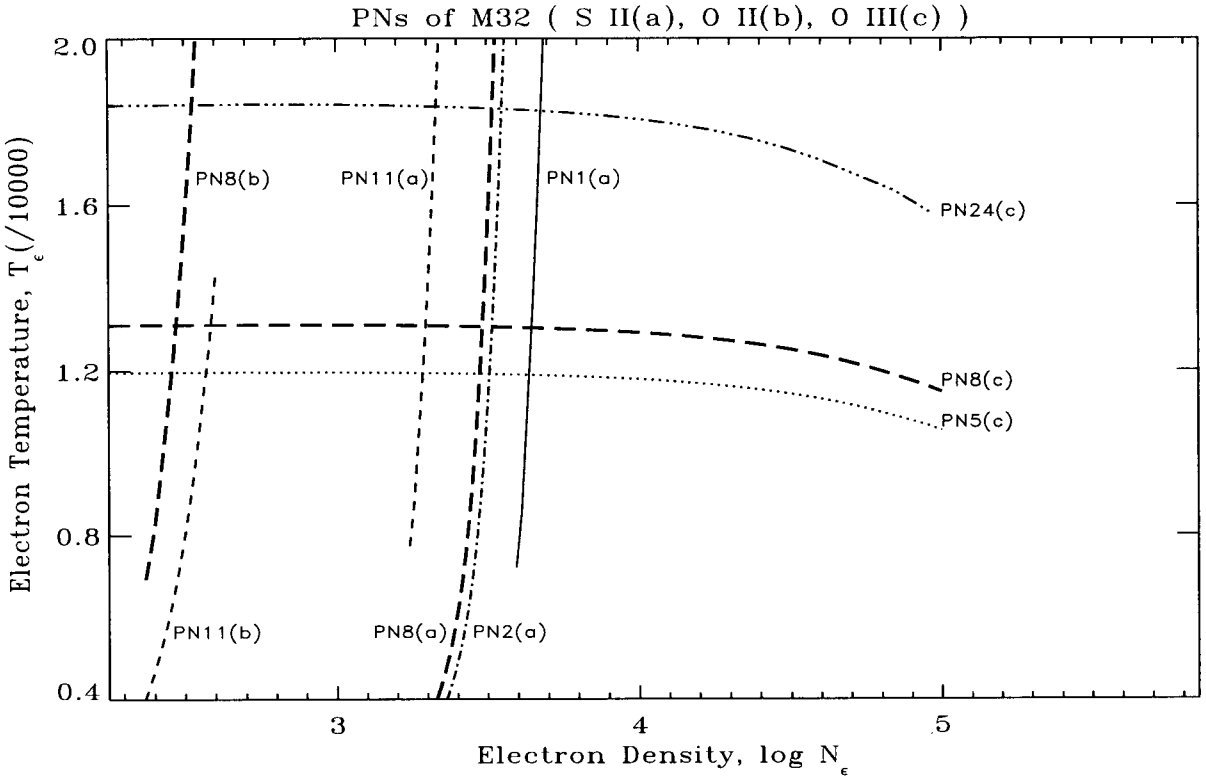

Fig. 2.— Temperatures of PNs in M 32. Temperatures vary from 9000 to 15 000 K.

abundances of M 31 largely differ from those of the Galactic PNs. O and Ne of M 31 PNs appear to more abundant than those in Galactic PNs. These PNs are likely to evolve from O-rich stars. Since the observed spectra data are not available for both C and N elements except for PN97, the given C and N abundances are only for references. Due to a small number of selected PNs, we cannot discuss any further as to whether the chemical abundances of M 31 differ from those of Galaxy.

In Table 4, for 4 PNs in M 31, we also present the model parameter of the planetary nebular nuclei (PNN, central star), i.e. effective temperatures and radius, as well. The PNN temperatures employed in the model 63 000, 70 000, 140 000, and 180 000 K for PN47, PN97, PN387, and PN17, respectively: the adopted H densities in the nebular shells are N_H = 8000, 9000, 6000 and 9000 atoms cm^{-3}

More numerous spectral lines are available in a more full wavelength coverage for M 32 PNs, i.e., wider wavelength coverage than for M 31. The observed emission lines in M 32 are [O II] 3727, [Ne III] 3869, H I, [O III] 4363/4959/5007, He I 4471/5876/6678, He II 4686, [N II] 5755/6548, [S II] 6717/6731, and [Ar III] 7135. The observed lines, available in M 32 PNs but not in M 31, are those of [O II], [N II], [S II], [Ar III]. The [O II]/[O III] lines would give a right excitation level information. Thus, we are able to determine these elemental abundances of M 32 PNs more correctly than those of M 31.

As in M 31, we used the spherically symmetric PN geometry for all PNs. The details of PN 32 model parameters, e.g., PNN and nebular shell, are given in Table 5. Similarly as in M 31 PNs modeling, we refer to the previous Galactic PN studies by Hyung et al. (see Table 3). These Galactic PNs provided a good starting point, i.e. initial input parameter for each PN modeling. The laborious trials have been done until we find a correct PNN parameter, i.e. central stellar temperature and the central stellar gravity, to fit the observed [O II]/[O III] line ratio and average gaseous electron temperature, etc. One, of course, must adjust chemical abundances, and physical parameter of nebula, i.e., size and density, in addition to the PNN parameter to find a satisfactory result.

In Table 5, we compare the predicted line intensities with the observed, similarly done for PNs in M 31 (see Table 4). Predictions for the lines of N, O, S, Ar and Ne seem generally successful. The predicted electron temperature and chemical abundances are also given at the bottom of Table 5. Theoretical prediction for T_e[O III] agrees fairly well with the diagnostic value for PN1, PN5, and PN7. The other PNs, i.e. PN6, PN8, PN24 and PN2 (highly uncertain [O III] 4363 emission nebula), PN11 and PN25 seem agreeable within the RSM error bars. RSM presented only the upper limit

Table 5-1.— Model predictions for PNs in M 32

Element	Wave	I_{obs}(PN1)	I_{cal1}	I_{cal2}	AVE	I_{obs}(PN8)	I_{cal1}	I_{cal2}	AVE
He I	5876	21.2	20.3	21.14		16.6	17.02	16.94	
He II	4686	10.8	.06	10.18					
N II	6584	230.6	226.49	230.53		168.2	170.23	168.72	
	6548	76.7	78.18	79.57		57.0	58.76	58.24	
O II	3726\	83	34.78	133.23		38.1	45.94	38.01	
	3729/		14.50	54.71		41.9	19.29	15.96	
O III	4959	337.8	340.23	345.38		462.5	485.69	491.19	
	5007	994.1	980.17	994.85		1386	1399.33	1415.15	
Ne III	3868	110.0	110.08	110.38		121	189.87	121.19	
	3969	49	32.85	32.92		62	56.68	36.17	
S II	6717	10.2	9.51	9.49		11.2	2.63	1.37	
	6731	17.08	17.17	17.40		17.1	4.68	2.56	
	6312					3.2	.89	.92	
	9069					13.2	15.34	14.12	
	9531					34.0	37.37	34.41	
Ar III	7136	18.0	17.16	18.05		18.0	19.34	18.49	
RSM	T_e	<11500				13000±1400			
OURS	T_e	12000				13000			
	N_e	4200				3200			
PNN	$R_\star$ ($R_\odot$)		0.35	0.1			0.55	0.55	
	$T_\star$(K)		85000	95000			90000	90000	
	log g		5.5	5.0			5.5	5.5	
Shell (pc)	R_{in}		0.005	0.03			0.005	0.005	
	R_{out}		0.066	0.038			0.092	0.097	
Prediction	T_e		10300	11600			10400	11200	
	N_e		8000	9000			8000	7500	
Chemical	He		1.30(-1)	1.38(-1)	1.34(-1)		1.10(-1)	1.08(-1)	1.09(-1)
Abundance	C		5.00(-5)	1.00(-4)	7.50(-5)		5.00(-5)	5.00(-5)	5.00(-5)
	N		3.50(-4)	9.70(-5)	2.24(-4)		3.10(-4)	3.21(-4)	3.16(-4)
	O	>2.6(-4)	3.30(-4)	3.13(-4)	3.22(-4)	2.4(-4)	4.80(-4)	3.80(-4)	4.30(-4)
	Ne		7.30(-5)	5.17(-5)	6.24(-5)		1.30(-4)	6.30(-5)	9.65(-5)
	S		2.00(-5)	6.20(-6)	1.31(-5)		6.30(-6)	4.96(-6)	5.63(-6)
	Ar		3.20(-6)	1.39(-6)	2.30(-6)		4.20(-6)	3.54(-6)	3.87(-6)

Table 5-2.— Model predictions for PNs in M 32

Element	Wave	I_{obs}(PN7)	I_{cal1}	I_{cal2}	AVE	I_{obs}(PN11)	I_{cal1}	I_{cal2}	AVE
He I	5876	14.0	14.29	14.00		17.1	16.59	16.14	
He II	4686	11.9	.87	11.94					
N II	6584	12.3	12.70	12.57		178.7	190.82	174.13	
	6548	5.7	4.38	4.34		60.3	65.87	60.11	
O II	3726\	25.2	27.85	149.18		123	22.10	45.55	
	3729/					119	10.05	21.53	
O III	4959	274.5	276.97	274.01		91.4	107.86	206.51	
	5007	805.8	797.92	789.26		298.4	310.73	594.89	
Ne III	3868	48	48.09	48.16		21	44.34	35.86	
	3969	21.3	14.35	14.37		16.5	13.23	10.70	
S II	6717					12.0	1.84	1.74	
	6731					16.3	3.13	2.85	
	9069					9.3	5.58	5.04	
Ar III	7136	5.5	5.48	5.74		8.5	10.55	9.32	
RSM	T_e	<13400				<25300			
OURS	T_e					12000			
	N_e					2000			
PNN	R_* ($R_\odot$)		0.65	0.09			0.25	0.25	
	T_*(K)		80000	93000			100000	100000	
	log g		5.0	5.0			5.5	5.5	
Shell (pc)	R_{in}		0.001	0.025			0.003	0.003	
	R_{out}		0.129	0.0455			0.089	0.095	
Prediction	T_e		12900	13500			17200	15800	
	N_e		4900	5000			6000	5000	
Chemical	He		8.80(-2)	9.30(-2)	9.05(-2)		9.00(-2)	9.00(-2)	9.00(-2)
Abundance	C		3.50(-4)	1.90(-4)	2.70(-4)		5.00(-5)	5.00(-5)	5.00(-5)
	N		1.75(-5)	3.98(-6)	1.07(-5)		9.00(-5)	9.00(-5)	9.00(-5)
	O	>1.3(-4)	1.45(-4)	1.71(-4)	1.58(-4)	>2.0(-5)	3.50(-5)	8.00(-5)	5.75(-5)
	Ne		1.55(-5)	1.43(-5)	1.49(-5)		7.50(-6)	7.50(-6)	7.50(-6)
	S		7.00(-7)	6.00(-7)	6.50(-7)		8.00(-7)	8.00(-7)	8.00(-7)
	Ar		7.00(-7)	3.65(-7)	5.33(-7)		7.50(-7)	7.50(-7)	7.50(-7)

Table 5-3.— Model predictions for PNs in M 32

Element	Wave	I_{obs}(PN5)	I_{cal1}	I_{cal2}	AVE	I_{obs}(PN2)	I_{cal1}	I_{cal2}	AVE
He I	5876	16.0	16.57	16.06		8.3	8.46	8.15	
He II	4686					22.8	1.62	22.77	
N II	6584	102.7	102.25	102.74		102.4	102.54	102.31	
	6548	29.6	35.29	35.46		30.9	35.39	35.32	
O II	3726\	29.0	72.10	21.17					
	3729/		30.67	8.77		85	43.34	51.94	
O III	4363	14.0	14.97	13.93					
	4959	431.7	433.51	448.45		508.7	507.75	508.51	
	5007	1291.8	1248.84	1291.82		1461.1	1462.70	1464.81	
Ne III	3868	94.0	94.28	94.41		98	98.18	98.33	
	3969	48.6	28.13	28.17		60	29.29	29.33	
S II	6717					9.0	3.25	3.73	
	6731					14.0	5.85	6.73	
	6312	10.4	.93	.87					
	9069	12.7	12.31	12.43		20.1	13.26	13.53	
	9531					32.2	32.31	32.96	
Ar III	7136	30.2	30.39	30.41		19.7	19.55	19.17	
RSM	T_e	11800±1300				<15700			
OURS	T_e	11600				12000			
	N_e	10000				3200			
PNN	R_* ($R_\odot$)		0.30	0.30			0.25	0.1	
	T_*(K)		80000	80000			80000	140000	
	log g		5.5	5.5			5.0	7.5	
Shell (pc)	R_{in}		0.003	0.003			0.005	0.025	
	R_{out}		0.056	0.051			0.056	0.053	
Prediction	T_e		12000	11500			13400	14800	
	N_e		8000	8000			8000	8000	
Chemical	He		1.00(-1)	1.00(-1)	1.00(-1)		5.00(-2)	6.60(-2)	5.80(-2)
Abundance	C		1.00(-4)	1.00(-4)	1.00(-4)		5.00(-5)	2.00(-4)	1.25(-4)
	N		8.60(-5)	2.94(-4)	1.90(-4)		6.54(-5)	5.20(-5)	5.87(-5)
	O	2.9(-4)	2.84(-4)	3.00(-4)	2.92(-4)	>1.9(-4)	2.66(-4)	2.72(-4)	2.69(-4)
	Ne		3.65(-5)	4.22(-5)	3.94(-5)		2.83(-5)	3.20(-5)	3.02(-5)
	S		2.80(-6)	3.50(-6)	3.15(-6)		2.65(-6)	2.40(-6)	2.53(-6)
	Ar		3.60(-6)	4.90(-6)	4.25(-6)		1.87(-6)	1.66(-6)	1.77(-6)

Table 5-4.— Model predictions for PNs in M 32

Element	Wave	I_{obs}(PN6)	I_{cal1}	I_{obs}(PN24)	I_{cal1}
He I	5876	29.6	29.71	22	22.41
He II	4686	32.0	32.72	39	40.97
N II	6584	42.0	42.10	268	268.05
	6548			94.7	92.53
O II	3726\	21.3	5.27	73	69.97
	3729/		2.16	48	29.02
O III	4363	23	17.39	47	41.58
	4959	598	601.09	572	574.38
	5007	1731	1731.33	1654	1654.67
Ne III	3868	127	127.46	134	134.11
	3969			54	40.01
S II	6717			9.5	3.46
	6731			11.4	6.28
	9069			17.5	17.50
Ar III	7136			17.3	17.32
RSM	T_e	12700±2500		18200±2500	
OURS	T_e			18300	
	N_e			10000	
PNN	R_* ($R_\odot$)		0.15		0.1
	T_*(K)		105000		180000
	log g		5.7		6.0
Shell (pc)	R_{in}		0.025		0.023
	R_{out}		0.0355		0.067
Prediction	T_e		10500		16500
	N_e		7000		8000
Chemical	He		2.24(-1)		1.71(-1)
Abundance	C		5.00(-5)		2.40(-5)
	N		1.12(-3)		2.21(-4)
	O	3.2(-4)	6.33(-4)	1.4(-4)	3.64(-4)
	Ne		1.19(-4)		7.23(-5)
	S		2.10(-6)		3.80(-6)
	Ar		1.00(-6)		2.43(-6)

Table 5-5.— Model predictions for PNs in M 32

Element	Wave	I_{obs}(PN25)	I_{cal1}	I_{cal2}	AVE	M32-PNs[1]	Ga-PNs[2]	Sun[3]
He I	5876	35.9	35.20	35.87				
N II	6584	159	159.49	159.31				
O III	4959	595	555.57	555.83				
	5007	1600	1600.25	1600.97				
Ne III	3868	152	152.70	152.67				
S II	9069	21.8	21.94	21.85				
RSM	T_e	<18600						
OURS	T_e							
	N_e							
PNN	R_* ($R_\odot$)		0.03	0.03				
	T_*(K)		165000	170000				
	log g		6.9	6.9				
Shell (pc)	R_{in}		0.027	0.031				
	R_{out}		0.033	0.0355				
Prediction	T_e		12200	12600				
	N_e		10000	10000				
Chemical	He		2.50(-1)	2.47(-1)	2.49(-1)	**1.36(-1)**	**1.11(-1)**	**0.98(-1)**
Abundance	C		9.00(-6)	4.60(-5)	2.75(-5)	**≥8.6(-5)**	**6.48(-4)**	**3.6(-4)**
	N		5.00(-5)	3.96(-5)	4.48(-5)	**2.53(-4)**	**1.40(-4)**	**1.1(-4)**
	O	>1.2(-4)	4.62(-4)	4.53(-4)	4.58(-4)	**3.31(-4)**	**4.93(-4)**	**8.5(-4)**
	Ne		6.41(-5)	5.51(-5)	5.96(-5)	**5.58(-5)**	**1.25(-4)**	**1.2(-4)**
	S		2.91(-6)	2.61(-6)	2.76(-6)	**3.84(-6)**	**8.08(-6)**	**1.6(-5)**
	Ar		8.00(-7)	9.00(-7)	8.50(-7)	**1.97(-6)**	**2.42(-6)**	**3.6(-6)**

[1]Average value for M 32 planetary nebulae. *C* abundance is the lower limit. [2] Average value for the Galactic PNs KB and also by AC83 (see text). [3] Solar abundance by Grevesse and Noels (1993).

for PN2, PN11 and PN25, while we derived the electron temperatures using the faint [O III] 4363 line. Due to the highly uncertain emission lines in PN2, the two model results are presented, which indicates very uncertain central star temperature, scattered by 50 000 K! Considering the diagnostics indication, it appears that the model with a relatively lower central star of $T_* =$ 80 000 K seems more appropriate.

Columns (7) and (8) in Table 5–5 compare the average abundances for M 32 PNs with the average value for the Galactic PN by KB and also by Aller and Czyzak (1983). The last column presents the solar abundance by Grevesse and Noels (1993). He and N abundances of M 32 PNs exceed those of the Galactic PN or the Sun, while the abundances of other elements do not exceed the average PN by KB or AC83 or the solar abundance.

In order of decreasing heavy element abundances (or the progenitor masses), PNs can be classified as Peimbert's (1978) types I (He and N rich), II (Intermediate Population I), III (high velocity) and IV (Halo population). The notable high abundances of H and N suggest that many M 32 PNs may belong to Peimbert's Type I. PN6 and PN24 have large He/H, and N/H ratios and these are probably of Peimbert Type I's. The central star temperatures are 105 000 and 180 000 K, respectively. These two PNs might evolve from progenitor stars that were more massive than the sun. See the typical Galactic PN, NGC 2440 of a Peimbert type I, of which He and N are enriched as compared with the sun or the average PNs. The high excitation PN24 might be one of the youngest PN in M 31. PN25 which has a large He/H ratio might be of Type I, as well.

The cats eye Galactic planetary nebula NGC 6543 has been known to have a WR type PNN and it appears to have a spatial gradient of He abundance, possibly a footprint of the recent mass outflow history. The central star of NGC 6543 is believed to consist of a pure He (e.g. He/H $\sim$ 60). PN6, PN24 and PN25 might be the similar ones.

As pointed out earlier, the diagnostics indicates that the electron temperatures of the M 32 PNs are rather high. Our study shows that the chemical abundances of the M 32 PNs are far less than those of the Galactic PNs or the Sun. Thus, the higher electron temperatures found in the M 32 PNs are primary due to a generally low metallicity of M 32 PN, or due to an inherent low metallicity of the host galaxy M 32.

IV. DISCUSSION

Since the PNs in M 31 and M 32 are faint, one might expect only the high excitation bright PNs in the nearby extra-galaxies. Our model investigation showed that RSM observed the low excitation PNs, as well. From our model analysis, we obtained (a) abundances and (b) central star parameters. We have not performed any detailed analysis of M 31 PNs because of a small number of spectral lines available. Jacoby & Ciardullo (1999) performed a more elaborate spectral data analysis for their M 31 PN spectral data and derived O abundances for bulge PNe that average [O/H] = –0.5 (i.e. a factor of 3 down from solar), while stars in the bulge have [Fe/H] $\simeq$ +0.23, 70% higher than the Sun (Worthey, Faber & Gonzalez 1992). This is in contrast to the expectation (dating back to the pioneering efforts of Spinrad & Taylor 1971) that the stars giving rise to the PNe would be metal-rich.

In our investigation, a spherically symmetrical geometry is assumed for all PNs. However, the real geometries of PNs often deviate from a spherical symmetry. For a relatively large nearby Galactic PN, where the observations were carried out on a small portion of the nebular image, this spherical symmetry assumption became a serious problem – see Hyung (1994). The spherical geometry assumed for M31 and M32 model PNs should not change our conclusion, or the chemical abundance determination, though, since the observed spectral lines represent the whole images of M31 and M32 PN. To predict the observed lines and the electron temperature correctly, one also must introduce the unobserved elemental abundances correctly in a model. Thus, the photoionization model enables us to set the upper limit to the unobservables. As shown in Table 4 and 5, our photoionization modeling effort was fairly successful in fitting the line intensities and electron temperatures within the observational error bars. However, one must await the availability of UV spectroscopy to determine the C abundance precisely.

With the upper limit value of C/H in our the model, we obtained the abundance of heavy elements, i.e., He/H, N/H, O/H, Ne/H, which showed that most PNs in M 32 appear to be of low metallicity (even the case of the high mass PN progenitor) and they must be originated from low-metallicity progenitors (AGB and M.S.). M 32 itself might be a chemically less enhanced galaxy, compared to the Galaxy. The highest electron temperature of M 31 is fairly lower than that of M 32 or the Galactic PNs. This relatively low electron temperatures in M 31 PNs might be indicative of highly enhanced chemical abundances in the galaxy. This disagrees with the O abundance derivation by Jacoby & Ciardullo. Only with the full data analysis with more data published in the literatures, one can get a more complete conclusion on the chemical enrichment history of M 31 PNs.

For a fairly large number of PNs in M 31 and M 32, one can construct HR diagrams for the central stars, which will allow us to investigate their evolution as a function of metallicity. By deriving the central star properties and adopting an initial-to-final mass relation (Vassiliadis & Wood 1994), we will also be able to compare the $\alpha-$element abundances of M 31 and M 32 PNs to the main-sequence turnoff ages of their progenitors and consequently, to trace the history of chemical enrichment in M 31 (see Dopita et al. 1997). We must await till we secure more spectral data, though.

This research was supported in part by the Korea MOST Star Grant No. Star 00-2-500-00, by the KOSEF Grant No. 1999-1-113-001-5, and by STScI Grant No. AR 06372-01 95A.

REFERENCES

Aller, L. H., & Czyzak, S. J. 1983, ApJS, 51, 211 (AC83)

Baade, W. 1955, AJ, 60, 151

Ciardullo, R., & Demarque, P. 1978, IAU Symposium, 80, 345

Ciardullo, R., Jacoby, G. H., Ford, H. C., & Neill, J. D. 1989, ApJ, 339, 53

Davies, R. L., Sadler, E. M., & Peletier, R. F. 1993, MNRAS, 262, 250

Dopita, M. A., Vassiliadis, D., Wood, P. R., Meatheringham, S., Harrington, J. P., Bohlin, R. C., Ford, J. C., Stecher, T. P., & Maran, S. P. 1997, ApJ, 474, 188

Feibelman, W. A., Hyung, S., & Aller, L. H. 1994, ApJ, 426, 653

Ford, H. C., & Jacoby, G. H. 1978, ApJ, 219, 437

Ford, H. C., & Jenner, D. C. 1975, ApJ, 202, 365

Grevesse, N., & Noels, A. 1993, in origin and Evolution of the Elements, ed. N. Prantzos, E. VangioniFlam, and M. Casse (Cambridge Univ. Press, p. 15)

Hyung, S. 1994, ApJS, 90, 119

Hyung, S. 1999, JKAS, 32, 55

Hyung, S., & Aller, L. H. 1995, MNRAS, 273, 973

Hyung, S., & Aller, L. H. 1996, MNRAS, 278, 551

Hyung, S., & Aller, L. H. 1997, ApJ, 491, 242

Hyung, S., & Aller, L. H. 1997, MNRAS, 292, 71

Hyung, S., & Aller, L. H. 1998, PASP, 110, 466

Hyung, S., Aller, L. H., & Feibelman, W. A. 1994, ApJS, 93, 465

Hyung, S., Aller, L. H., & Feibelman, W. A. 1994, MNRAS, 269, 975

Hyung, S., Aller, L. H., & Feibelman, W. A. 1994, PASP, 106, 745

Hyung, S., Aller, L. H., & Feibelman, W. A. 1996, PASP, 108, 488

Hyung, S., Aller, L. H., & Feibelman, W. A. 1999, ApJ, 514, 878

Hyung, S., Keyes, C. D., & Aller, L. H. 1995, MNRAS, 272, 973

Hyung, S., Aller, L. H., Feibelman, W. A., Lee, W, & de Alex, A. 2000, MNRAS, in press

Hubeny, I. 1988, Computer Phys. Comm., 52, 103

Jacoby, G. H., & Ciardullo, R. 1999, ApJ, 515, 169

Kingsburgh, R. L., & Barlow, M. J. 1994, MNRAS, 271, 257 (KB)

McCarthy, J. K., Kudritzki, R. P., Lennon, D. J. et al. 1997, ApJ, 482, 757

Pagel, B. E. J., & Edmunds, M. G. 1981, ARA&A, 19, 77

Peimbert, M. 1978, in IAU Symposium No. 76, Planetary Nebulae, Observations and Theory, ed. Y. Terzian (Dordrecht: D. Reidel), 215

Richer, M. G., Stasinks, G., & McCall, M. L. 1999, A&AS, 135, 203

Spinrad, J., & Taylor, B. 1971, ApJS, 22, 445

Vassiliadis, E., & Wood, P. R. 1994, ApJS, 92, 125

Walsh, J. R., & Roy, J. -R. 1989, MNRAS, 239, 297

Walsh, J. R., Walton, N. A., Jacoby, G. J., & Peletier, R. F. 1999, A&A, 346, 753

Worthey, G., Faber, S. M., & Gonzalez, J. J. 1992, ApJ, 398, 69